Acta Cryst E CRYSTALLOGRAPHIC COMMUNICATIONS

ISSN 2056-9890

Crystal structure of spinel-type $Li_{0.64}Fe_{2.15}Ge_{0.21}O_4$

Günther J. Redhammer* and Gerold Tippelt

University of Salzburg, Department Chemistry and Physics of Materials, Hellbrunnerstrasse 34, 5020 Salzburg, Austria. *Correspondence e-mail: guenther.redhammer@sbg.ac.at

Received 1 March 2016
Accepted 11 March 2016

Edited by M. Weil, Vienna University of Technology, Austria

Keywords: crystal structure; spinel; Mössbauer spectroscopy; geoscience.

CCDC reference: 1463892

Supporting information: this article has supporting information at journals.iucr.org/e

Spinel-type $Li_{0.64}Fe_{2.15}Ge_{0.21}O_4$, lithium diiron(III) germanium tetraoxide, has been formed as a by-product during flux growth of an Li–Fe–Ge pyroxene-type material. In the title compound, lithium is ordered on the octahedral *B* sites, while Ge^{4+} orders onto the tetrahedral *A* sites, and iron distributes over both the octahedral and tetrahedral sites, and is in the trivalent state as determined from Mössbauer spectroscopy. The oxygen parameter *u* is 0.2543; thus, the spinel is close to having an ideal cubic closed packing of the O atoms. The title spinel is compared with other Li- and Ge-containing spinels.

1. Chemical context

The minerals of the spinel group are widely occurring compounds in the geosphere and are important not only in geoscience but also in many other disciplines. In recent years, in particular, Li-containing spinels like $LiMn_2O_4$ or $Li_{0.5}Fe_{2.5}O_4$ have attracted much interest in battery technology as possible candidates for cathode materials in lithium ion secondary batteries (Liu *et al.*, 2014; Patil *et al.*, 2016; Thackeray *et al.*, 1983). The ideal spinel structure consists of a closed packing of anions *X*, with one-eighth of the tetrahedral interstices and one-half of the octahedral interstices occupied by the cations. The vast majority of spinels crystallize in the space group $Fd\overline{3}m$. Here the cations in tetrahedral coordination occupy special position 8*a* (point symmetry $\overline{4}3m$, at $\frac{1}{8}, \frac{1}{8}, \frac{1}{8}$), while the octahedrally coordinated cations reside on special position 16*d* (point symmetry $\overline{3}m$ at $\frac{1}{2}, \frac{1}{2}, \frac{1}{2}$). The anions are at equipoint position 32*e*, which requires one positional parameter, often denoted as the *u* parameter. For $u = 0.25$, an ideal cubic closed packing of anions is realized and the octahedral bond length is 1.155 times larger than the tetrahedral one. Following Hill *et al.* (1979), variations in *u* reflect the adjustment of the structure to accommodate cations of different size in octahedral and tetrahedral positions. Increasing the value of *u* above 0.25 moves the anions away along [111] from the nearest tetrahedral cation, thereby increasing the size of the tetrahedron at the extent of the size of the octahedron. The majority of the spinels can be described with the general formula AB_2O_4, with the *A* and *B* cations having the formal charges $A = 2$ and $B = 3$ (2,3 spinels) or $A = 4$ and $B = 2$ (4,2 spinels). The perfect *normal* spinel is one in which the single *A* cation occupies the tetrahedral site and the two *B* cations reside at the two equivalent octahedral positions. Introducing parentheses, *i.e.* (. . .) and brackets, *i.e.* [. . .], for tetrahedral and octahedral coordination, respectively, one may write the normal spinels in the form $(A)[B_2]O_4$. In contrast, the complete inverse spinel has a cationic distribution of $(B)[AB]O_4$ (O'Neill & Navrotsky, 1983). More detailed reviews on the spinel structure and crystal chemistry can be

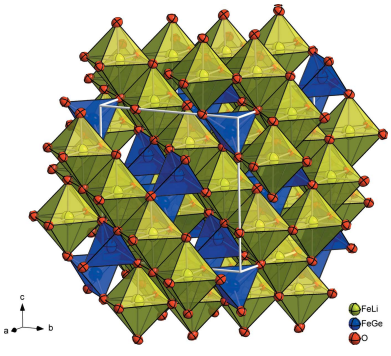

found, for example, in Biagioni & Pasero (2014), Harrison & Putnis (1998), Hill *et al.* (1979) and O'Neill & Navrotsky (1983).

Germanium-containing spinels are considered to belong to the normal spinels, with a full ordering of Ge^{4+} onto the tetrahedral *A* site, while metal cations *M* order onto the octahedral *B* sites. This was demonstrated by, among others, Von Dreele *et al.* (1977) for $GeMg_2O_4$ and Welch *et al.* (2001) for the mineral brunogeierite ($GeFe_2O_4$). For $LiMn_2O_4$ and $LiNi_{0.5}Mn_{1.5}O_4$, which represent excellent cathode materials, it was found that Li^+ orders onto the tetrahedral site (Berg *et al.*, 1998; Liu *et al.*, 2014). Also for $LiCrGeO_4$, Touboul & Bourée (1993) reported an almost exclusive ordering of Li^+ for the tetrahedral site, while Cr^{3+} and Ge^{4+} occupy the octahedral sites. Different to this is the spinel $Li_{0.5}Fe_{2.5}O_4$. This compound is an inverse spinel in which Fe^{3+} is ordered onto the tetrahedral site, while Li^+ and the remaining Fe^{3+} are distributed over the octahedral site (Hankare *et al.*, 2009; Patil *et al.*, 2016; Tomas *et al.*, 1983). This cationic distribution is thus similar to that in the inverse spinel magnetite, $FeFe_2O_4$ (Fleet, 1981).

During the synthesis of Li–Fe–Ge pyroxenes (Redhammer *et al.*, 2009, 2010), black octahedral-shaped single crystals were frequently obtained, which turned out to be a spinel-type compound with significant Li^+ and small Ge^{4+} concentrations. We present here the structure refinement and ^{57}Fe Mössbauer spectroscopic characterization of these crystals.

2. Structural commentary

The structure of the title compound is shown in Fig. 1. The site-occupation refinement indicates that Li^+ orders onto the octahedral *B* site, while Ge^{4+} is found on the tetrahedral *A* site, indicating a partial inverse spinel arrangement; iron is distributed over both sites. The derived crystal chemical formula of the title compound is thus $(Fe^{3+}_{0.79}Ge^{4+}_{0.21})$-$[Li^+_{0.64}Fe^{3+}_{1.36}]O_4$, with the valence state of iron determined from ^{57}Fe Mössbauer spectroscopy (see below). This formula is balanced in charge and agrees very well with the chemical composition determined from electron microprobe analysis. Generally, the title compound is similar to the $Li_{0.5}Fe_{2.5}O_4$ spinel-type materials. The shift of Li^+ to the octahedral site, for example, in comparison with $LiCrGeO_4$ or $LiMn_2O_4$, can be explained by the strong preference of Fe^{3+} for the tetrahedral site. Based on the concept of crystal field stabilization energy, Miller (1959) theoretically calculated octahedral site preference energies which gave a stronger preference of Fe^{3+} for the tetrahedral site as compared, for example, to Li^+ or Mn^{3+}.

The lattice parameter of the title compound [8.2903 (3) Å] is smaller in comparison with, for example, magnetite Fe_3O_4 [a = 8.3941 (7) Å; Fleet, 1981], but larger than that observed in the Li spinels $LiCrGeO_4$ [a = 8.1976 (1) Å; Touboul & Bourée, 1993] or $LiMn_2O_4$ and $LiNi_{0.5}Mn_{1.5}O_4$ (a = 8.243 and 8.1685 Å, respectively; Liu *et al.*, 2014). This is due mainly to the high amount of Fe^{3+} at the *A* sites, which has a larger ionic radius than Ge^{4+}, Ni^{3+} or $Mn^{3+/4+}$ (Shannon & Prewitt, 1969). The oxygen parameter u = 0.2543 is close to the ideal value for cubic closed packing, reflecting some distinct differences to the spinels which have the *A* site fully occupied by Li^+. In the title compound, the bond length of the tetrahedrally coordinated site *T* is 1.857 (2) Å, which is distinctly smaller than in, for example, $LiMn_2O_4$, with the tetrahedral site being fully occupied by Li^+. The *T*—O bond length is also smaller than in magnetite (Fleet, 1981) or $Li_{0.5}Fe_{2.5}O_5$ (Tomas *et al.*, 1983), with values of 1.8889 (9) and 1.880 (5) Å, respectively. In $GeFe_2O_4$, the *T*—O bond length is only 1.771 (2) Å and this smaller value of *T*—O compared to, for example, magnetite is due to the substitution of Ge^{4+} onto the *A* site and can be seen as additional proof for the correctness of the derived cationic distribution.

The bond length involving the octahedrally coordinated site *M* is 2.0373 (11) Å, which is 1.07 times larger than the bond length involving the tetrahedrally coordinated site. The *M*—O

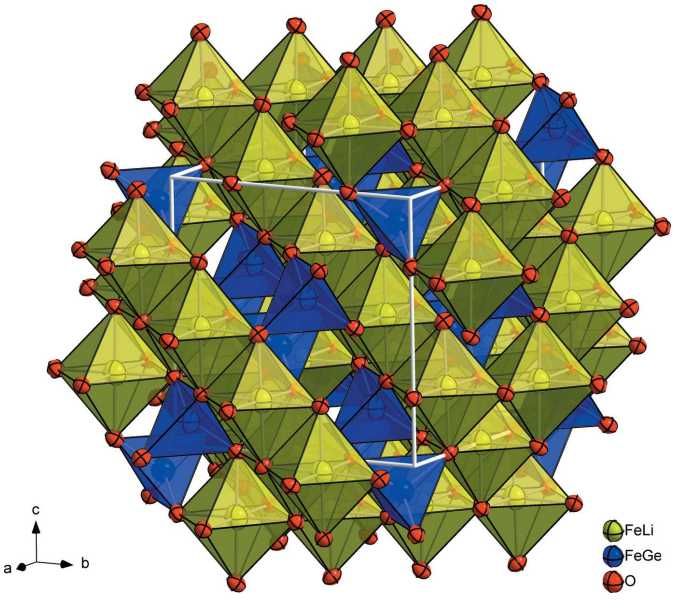

Figure 1
Polyhedral drawing of the spinel-type structure of the title compound. Anisotropic displacement parameters are drawn at the 95% probability level.

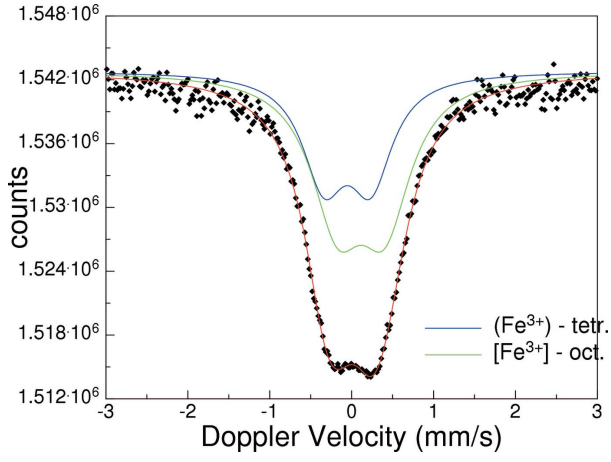

Figure 2
^{57}Fe Mössbauer spectrum of the title compound, recorded at 740 K.

Table 1
Experimental details.

Crystal data	
Chemical formula	$Li_{0.64}Fe_{2.15}Ge_{0.21}O_4$
M_r	203.5
Crystal system, space group	Cubic, $Fd\bar{3}m$
Temperature (K)	298
a (Å)	8.2903 (3)
V (Å^3)	569.78 (6)
Z	8
Radiation type	Mo $K\alpha$
μ (mm^{-1})	12.85
Crystal size (mm)	0.13 × 0.12 × 0.12
Data collection	
Diffractometer	Bruker SMART APEX CCD
Absorption correction	Multi-scan (*SADABS*; Bruker, 2012)
T_{min}, T_{max}	0.83, 0.94
No. of measured, independent and observed [$I > 2\sigma(I)$] reflections	3046, 118, 114
R_{int}	0.021
(sin $\theta/\lambda)_{max}$ (Å^{-1})	0.940
Refinement	
$R[F^2 > 2\sigma(F^2)]$, $wR(F^2)$, S	0.018, 0.042, 1.37
No. of reflections	118
No. of parameters	10
No. of restraints	1
$\Delta\rho_{max}$, $\Delta\rho_{min}$ (e Å^{-3})	0.36, −0.67

Computer programs: *APEX2* and *SAINT* (Bruker, 2012), *SHELXL2014* (Sheldrick, 2015), *DIAMOND* (Brandenburg, 2006) and *WinGX* (Farrugia, 2012).

bond length is somewhat larger than 2.025 (3) Å in $Li_{0.5}Fe_{2.5}O_4$ (Tomas *et al.*, 1983). This agrees well with the observed higher Li content in the title compound, with the ionic radius for Li^+ in an octahedral coordination (0.740 Å) being larger than that of Fe^{3+} (0.645 Å; Shannon & Prewitt, 1969), thus increasing the M—O distance. Magnetite has a mixed occupation of the octahedral sites, with both Fe^{2+} and Fe^{3+}, thus having a larger M—O bond length of 2.0582 (9) Å, while in $GeFe_2O_4$, all the Fe atoms are in a divalent state and an M—O bond length of 2.132 (2) Å is observed.

In order to quantify the valence state of iron in the title compound, a ^{57}Fe Mössbauer spectrum was recorded at 340 K. It shows a broad, slightly asymmetric, doublet, which can be evaluated with two Lorentzian-shaped doublets (Fig. 2). The first doublet shows an isomer shift (IS) of −0.053 (17) mm s^{-1} and a quadrupole splitting (QS) of 0.57 (3) mm s^{-1}, and can be assigned to the ferric iron on the tetrahedral site. The second doublet has a larger IS of 0.115 (14) mm s^{-1} and an almost identical QS of 0.58 (2) mm s^{-1}, and is assigned to ferric iron at the octahedral site. No indications for ferrous iron are present. The QS values suggest low polyhedral distortion, which is almost identical in both sites. The relative area ratio of tetrahedral to octahedral sites is 38.6 (8) to 61.4 (9)%. Assuming a total amount of 2.15 formula units Fe^{3+}, the results of Mössbauer spectroscopy give a cation distribution of $(Fe^{3+}_{0.83})[Fe^{3+}_{1.32}]$, which is in good agreement with that obtained from the site-occupation refinement of the X-ray data. At room temperature, the title compound is magnetically ordered, as revealed by its ^{57}Fe Mössbauer spectrum.

3. Synthesis and crystallization

The spinel formed as a by-product during the synthesis of pyroxene-type $LiFeGe_2O_6$ in flux-growth experiments (Redhammer *et al.*, 2010). For the synthesis of the pyroxene, Li_2CO_3, Fe_2O_3 and GeO_2 in the stoichiometry of the compound and $Li_2MoO_4/LiVO_3$ as a flux (mass ratio sample to flux = 1:10) were mixed together, heated to 1473 K in a platinum crucible, covered with a lid, held at this temperature for 24 h and cooled afterwards at a rate of 1.5 K h^{-1} to 973 K. The experimental batch consisted of large pyroxene crystals and a distinct amount of black crystals with idiomorphic octahedral habit, up to 200 µm. Semi-quantitative EDX (energy-dispersive X-ray) analysis revealed iron and some germanium as the main elements; powder X-ray diffraction analysis revealed the crystals as a spinel-type material. An electron microprobe analysis on polished/embedded crystals (three different grains with five measurement points each) yielded a chemical composition of 84.86 (30) wt% Fe_2O_3, 10.52 (25) wt% GeO_2 and 4.62 wt% Li_2O, with the latter calculated from the difference to 100 oxide%. There is no evidence for Mo or V from the flux, nor for any other chemical elements. From the oxide percentage, a chemical formula of $Li_{0.63\,(2)}Fe_{2.18\,(1)}Ge_{0.20\,(2)}O_4$ was calculated, which is in good agreement with that obtained from the structure refinement. Individual crystals are homogeneous in composition, with no significant systematic variation from rim-core; also, there is no systematic variation in composition from crystal to crystal.

4. Refinement

Crystal data, data collection and structure refinement details are summarized in Table 1. In a first stage of refinement, only iron was considered on the A and B sites, thereby allowing unconstrained refinement of the site-occupation factors. This gave a surplus of electron density (higher occupation than allowed by the multiplicity) at the tetrahedral site, while a lower occupation than possible was found for the octahedral site. From this it was concluded that Li enters the octahedral site and Ge enters the tetrahedral site. In the final refinements, it was assumed that both tetrahedral and octahedral sites are fully occupied, with Fe + Ge = 1 as a restraint for the tetrahedral site and Fe + Li = 1 for the octahedral site.

References

Berg, H., Thomas, J. O., Liu, W. & Farrington, G. C. (1998). *Solid State Ionics*, **112**, 165–168.
Biagioni, C. & Pasero, M. (2014). *Am. Mineral.* **99**, 1254–1264.
Brandenburg, K. (2006). *DIAMOND*. Crystal Impact GbR, Bonn, Germany.
Bruker (2012). *APEX2*, *SAINT* and *SADABS*. Bruker AXS Inc., Madison, Wisconsin, USA.
Farrugia, L. J. (2012). *J. Appl. Cryst.* **45**, 849–854.
Fleet, M. E. (1981). *Acta Cryst.* B**37**, 917–920.
Hankare, P. P., Patil, R. P., Sankpal, U. B., Jadhav, S. D., Lokhande, P. D., Jadhav, K. M. & Sasikala, R. (2009). *J. Solid State Chem.* **182**, 3217–3221.
Harrison, R. J. & Putnis, A. (1998). *Surv. Geophys.* **19**, 461–520.

Hill, R. J., Craig, J. R. & Gibbs, G. V. (1979). *Phys. Chem. Miner.* **4**, 317–339.
Liu, D., Zhu, W., Trottier, J., Gagnon, C., Barray, F., Guerfi, A., Mauger, A., Groult, H., Julien, C. M., Goodenough, J. B. & Zaghib, K. (2014). *RSC Adv.* **4**, 154–167.
Miller, A. (1959). *J. Appl. Phys.* **30**, S24–S25.
O'Neill, H. S. C. & Navrotsky, A. (1983). *Am. Mineral.* **68**, 181–194.
Patil, R. P., Patil, S. B., Jadhav, B. V., Delekar, S. D. & Hankare, P. P. (2016). *J. Magn. Magn. Mater.* **401**, 870–874.
Redhammer, G. J., Cámara, F., Alvaro, M., Nestola, F., Tippelt, G., Prinz, S., Simons, J., Roth, G. & Amthauer, G. (2010). *Phys. Chem. Miner.* **37**, 685–704.
Redhammer, G. J., Roth, G., Treutmann, W., Hoelzel, M., Paulus, W., André, G., Pietzonka, C. & Amthauer, G. (2009). *J. Solid State Chem.* **182**, 2374–2384.
Shannon, R. D. & Prewitt, C. T. (1969). *Acta Cryst.* B**25**, 925–946.
Sheldrick, G. M. (2015). *Acta Cryst.* C**71**, 3–8.
Thackeray, M. M., David, W. I. F., Bruce, P. G. & Goodenough, J. B. (1983). *Mater. Res. Bull.* **18**, 461–472.
Tomas, A., Laruelle, P., Dormann, J. L. & Nogues, M. (1983). *Acta Cryst.* C**39**, 1615–1617.
Touboul, M. & Bourée, F. (1993). *J. Mater. Chem.* **3**, 623–626.
Von Dreele, R. B., Navrotsky, A. & Bowman, A. L. (1977). *Acta Cryst.* B**33**, 2287–2288.
Welch, M. D., Cooper, M. A. & Hawthorne, F. C. (2001). *Mineral. Mag.* **65**, 441–444.

supporting information

Acta Cryst. (2016). E**72**, 505-508 [https://doi.org/10.1107/S205698901600414X]

Crystal structure of spinel-type $Li_{0.64}Fe_{2.15}Ge_{0.21}O_4$

Günther J. Redhammer and Gerold Tippelt

Computing details

Data collection: *APEX2* (Bruker, 2012); cell refinement: *SAINT* (Bruker, 2012); data reduction: *SAINT* (Bruker, 2012); program(s) used to solve structure: coordinates from an isotypic structure; program(s) used to refine structure: *SHELXL2014* (Sheldrick, 2015); molecular graphics: *DIAMOND* (Brandenburg, 2006); software used to prepare material for publication: *WinGX* (Farrugia, 2012).

Lithium diiron(III) germanium tetraoxide

Crystal data

$Li_{0.64}Fe_{2.15}Ge_{0.21}O_4$
M_r = 203.5
Cubic, $Fd\bar{3}m$
Hall symbol: -F 4vw 2vw 3
a = 8.2903 (3) Å
V = 569.78 (6) Å^3
Z = 8
$F(000)$ = 771
D_x = 4.744 Mg m^{-3}
Mo $K\alpha$ radiation, λ = 0.71073 Å
Cell parameters from 3046 reflections
θ = 7.0–41.9°
μ = 12.85 mm^{-1}
T = 298 K
Octahedron, black
0.13 × 0.12 × 0.12 mm

Data collection

Bruker SMART APEX CCD diffractometer
Radiation source: 3-circle diffractometer
Graphite monochromator
ω–scan at 4 different φ positions
Absorption correction: multi-scan (*SADABS*; Bruker, 2012)
T_{min} = 0.83, T_{max} = 0.94
3046 measured reflections
118 independent reflections
114 reflections with $I > 2\sigma(I)$
R_{int} = 0.021
θ_{max} = 41.9°, θ_{min} = 7.0°
h = −15→14
k = −14→10
l = −15→13

Refinement

Refinement on F^2
Least-squares matrix: full
$R[F^2 > 2\sigma(F^2)]$ = 0.018
$wR(F^2)$ = 0.042
S = 1.37
118 reflections
10 parameters
1 restraint
$w = 1/[\sigma^2(F_o^2) + (0.0139P)^2 + 2.542P]$ where $P = (F_o^2 + 2F_c^2)/3$
$(\Delta/\sigma)_{max} < 0.001$
$\Delta\rho_{max}$ = 0.36 e Å^{-3}
$\Delta\rho_{min}$ = −0.67 e Å^{-3}
Extinction correction: SHELXL2014 (Sheldrick, 2015)
Extinction coefficient: 0.0051 (6)

Special details

Geometry. All esds (except the esd in the dihedral angle between two l.s. planes) are estimated using the full covariance matrix. The cell esds are taken into account individually in the estimation of esds in distances, angles and torsion angles; correlations between esds in cell parameters are only used when they are defined by crystal symmetry. An approximate (isotropic) treatment of cell esds is used for estimating esds involving l.s. planes.

Fractional atomic coordinates and isotropic or equivalent isotropic displacement parameters (Å²)

	x	*y*	*z*	U_{iso}*/U_{eq}	Occ. (<1)
Fe1	0.5	0.5	0.5	0.00795 (17)	0.678 (4)
Li1	0.5	0.5	0.5	0.00795 (17)	0.322 (4)
Fe2	0.125	0.125	0.125	0.00573 (17)	0.795 (3)
Ge2	0.125	0.125	0.125	0.00573 (17)	0.205 (3)
O2	0.25434 (14)	0.25434 (14)	0.25434 (14)	0.0095 (3)	

Atomic displacement parameters (Å²)

	U^{11}	U^{22}	U^{33}	U^{12}	U^{13}	U^{23}
Fe1	0.00795 (17)	0.00795 (17)	0.00795 (17)	−0.00100 (11)	−0.00100 (11)	−0.00100 (11)
Li1	0.00795 (17)	0.00795 (17)	0.00795 (17)	−0.00100 (11)	−0.00100 (11)	−0.00100 (11)
Fe2	0.00573 (17)	0.00573 (17)	0.00573 (17)	0	0	0
Ge2	0.00573 (17)	0.00573 (17)	0.00573 (17)	0	0	0
O2	0.0095 (3)	0.0095 (3)	0.0095 (3)	0.0010 (3)	0.0010 (3)	0.0010 (3)

Geometric parameters (Å, º)

Fe1—O2^{i}	2.0373 (11)	Fe1—Fe1^{ii}	2.9311 (1)
Fe1—O2^{ii}	2.0373 (11)	Fe2—O2^{vii}	1.857 (2)
Fe1—O2^{iii}	2.0373 (11)	Fe2—O2^{viii}	1.857 (2)
Fe1—O2^{iv}	2.0373 (11)	Fe2—O2^{ix}	1.857 (2)
Fe1—O2^{v}	2.0373 (11)	Fe2—O2	1.857 (2)
Fe1—O2^{vi}	2.0373 (11)		
O2^{i}—Fe1—O2^{ii}	180	O2^{ii}—Fe1—O2^{vi}	87.96 (7)
O2^{i}—Fe1—O2^{iii}	87.96 (7)	O2^{iii}—Fe1—O2^{vi}	92.04 (7)
O2^{ii}—Fe1—O2^{iii}	92.04 (7)	O2^{iv}—Fe1—O2^{vi}	87.96 (7)
O2^{i}—Fe1—O2^{iv}	92.04 (7)	O2^{v}—Fe1—O2^{vi}	180.00 (7)
O2^{ii}—Fe1—O2^{iv}	87.96 (7)	O2^{vii}—Fe2—O2^{viii}	109.5
O2^{iii}—Fe1—O2^{iv}	180	O2^{vii}—Fe2—O2^{ix}	109.5
O2^{i}—Fe1—O2^{v}	87.96 (7)	O2^{viii}—Fe2—O2^{ix}	109.5
O2^{ii}—Fe1—O2^{v}	92.04 (7)	O2^{vii}—Fe2—O2	109.4710 (10)
O2^{iii}—Fe1—O2^{v}	87.96 (7)	O2^{viii}—Fe2—O2	109.5
O2^{iv}—Fe1—O2^{v}	92.04 (7)	O2^{ix}—Fe2—O2	109.4710 (10)
O2^{i}—Fe1—O2^{vi}	92.04 (7)		

Symmetry codes: (i) *x*+1/4, *y*+1/4, −*z*+1; (ii) −*x*+3/4, −*y*+3/4, *z*; (iii) *x*+1/4, −*y*+1, *z*+1/4; (iv) −*x*+3/4, *y*, −*z*+3/4; (v) −*x*+1, *y*+1/4, *z*+1/4; (vi) *x*, −*y*+3/4, −*z*+3/4; (vii) −*x*+1/4, *y*, −*z*+1/4; (viii) *x*, −*y*+1/4, −*z*+1/4; (ix) −*x*+1/4, −*y*+1/4, *z*.